"Reason, Observation, and
Experience—the Holy Trinity of Science".

***Robert G. Ingersoll** (1833–1899), U.S. lawyer.*
The Gods.

CHAPTER 6

COMPOUNDING: PRODUCTION OF PANIPOL™-SBS BLENDS

6.1 INTRODUCTION.

As has been seen, preliminary results suggested that melt mixing in a batch mixer (section 5.2.4) was the most favourable technique to incorporate the PANIPOL^{TM} complex with the polymer matrices. Consequently, this chapter describes the modifications performed to this compounding method in order to enhance the level of homogeneity in the blends. As also seen, preliminary results from the morphological analyses revealed that the polyaniline phase can deform under favourable conditions into uniform and continuous elongated domains, preferentially oriented in the extrusion direction, in extrudates in which the polymer matrix was SBS (section 5.5.3). As a result, the research concentrates now on the system PANIPOL^{TM}2-SBS. In order to investigate the behaviour of the conductivity with respect to composition, electrical resistance measurements were performed on blends containing 5, 10, 15, 20, 35 and 50 weight percent of the conductive complex. The experiments are also detailed here in the relevant section. Finally, the morphology of the blends was analysed following different microscopy techniques. As in all the experimental methods described in this chapter, a general account of the details of each technique employed will be presented followed by the results following from them. General conclusions are also presented at the end of the chapter.

6.2 BLENDS PREPARATION.

The compounding was performed using the batch mixer described in section 5.2.4 at 130°C. The modifications performed to the compounding method to enhance the homogeneity of the blends included:

- Speed of the rotors during the feed of the polymer matrix (stage 2). This was set at 2 rpm.
- Compounding speed (stage 6). The speed of the rotors was set at 15 rpm.
- Compounding time (stage 8). The compounding was carried out for 5 min.

The rest of the compounding sequence was the same. For information on the details, the reader is invited to consult the original sequence described in section 5.2.4.

On the other hand, the nomenclature used to identify the blends is indicated in Table 6.1.

Table 6.1. Nomenclature used for the PANIPOL™2-SBS blends.

wt.% of PANIPOL™	**Nomenclature**
5	5PANIPOL/SBS
10	10PANIPOL/SBS
15	15PANIPOL/SBS
20	20PANIPOL/SBS
35	35PANIPOL/SBS
50	50PANIPOL/SBS

Again, for practical and safety reasons, three batches of 40 g each were used in the preparation of each blend. The raw materials were used as received and the blends produced were properly stored to await further experimentation.

The dispersion of PANIPOL™ in the blends improved considerably due to the increase of the shear stresses occurring in the melt, which resulted from the increase of the rotors' speed. In addition, the conductive complex was given more time to mix properly with the polymer matrix. All this was reflected in the increase of the torque during the production of the blends (Table 6.2).

Table 6.2. Torque levels during the production of the blends.

BLENDS	**TORQUE (Nm)**	
	STAGE 6	**STAGE 8**
5PANIPOL/SBS	37-39	29-31
10PANIPOL/SBS	34-36	27-29
15PANIPOL/SBS	32-34	22-24
20PANIPOL/SBS	30-33	18-20
35PANIPOL/SBS	23-26	14-16
50PANIPOL/SBS	14-17	13-16

As can be seen in Table 6.2, the torque levels during the preparation of the blends were higher than those observed when lower compounding speed and time, respectively, were used to prepare blends of comparable compositions and batch sizes (Table 5.2 in chapter 5). Again, stage 6 in Table 6.2 refers to the compounding stage in

which only the polymer matrix, already in its molten sate, was into the mixing chamber. On the other hand, stage 8 refers to the stage in which the compounding was actually taking place. As previously observed, the torque decreased after adding PANIPOL™ to the polymer matrices because this complex is less viscous than SBS and also acts as a processing aid in lowering the melt viscosity of the blends.

Table 6.2 also shows that the torque levels decreased with the increase of the conductive complex in the blends, the main reason being that the blends were becoming less viscous with the increase in PANIPOL™ content. On the other hand, since batches of the same size (i.e., 40 g) were used in the preparation of all the blends regardless of their composition, which is not strictly correct, it is likely that the homogeneity degree of the blends also decreased with the increase of the PANIPOL™ content. As has already been explained, the batch size is a function of the blend composition (refer to section 5.2.4), which can be estimated by using the fill factor principle [186]. To illustrate this, Table 6.3 presents the optimum batch size corresponding to each blend, which was calculated by using the maximum and minimum values recommended for the fill factor, equations 5.1 to 5.4 (from section 5.2.4) and the density values for PANIPOL™ and SBS (refer to chapter 3).

Table 6.3. Optimum batch sizes calculated for the blends PANIPOL™-SBS.

BLENDS	**BATCH SIZES (g)**	
	Fill factor = 0.7	**Fill factor = 0.8**
5PANIPOL/SBS	39.77	45.45
10PANIPOL/SBS	40.06	45.79
15PANIPOL/SBS	40.36	46.13
20PANIPOL/SBS	40.66	46.47
35PANIPOL/SBS	41.60	47.54
50PANIPOL/SBS	42.58	48.66

As can be seen in Table 6.3, the optimum batch size corresponding to each blend should increase with the increase of PANIPOL™ in the blends. In consequence, the torque levels that would be generated by using the correct batch size would be higher than those presented in Table 6.2 (stage 8). Again, as has already been mentioned

before, batches of 40 g were used in the preparation of all the blends due to practical and safety reasons.

The temperature of the melt during the final compounding stage (stage 8) increased with respect to the temperature originally set for the mixing chamber (130°C). The increment of temperature (ΔT) varied. This is presented for each blend in Table 6.4.

Table 6.4. Increment of temperature (ΔT) of the blends during the final compounding stage.

BLENDS	**ΔT (^{o}C)**
5PANIPOL/SBS	16-24
10PANIPOL/SBS	13-16
15PANIPOL/SBS	11-16
20PANIPOL/SBS	3-15
35PANIPOL/SBS	5-8
50PANIPOL/SBS	9-10

As can be seen in Table 6.4, the increment of temperature was higher than that observed (1-4°C, section 5.2.4) when lower compounding speed and time, respectively, were used. This is due to the increase of the frictional heat generated by the shear action of the rotors because of the increase of their rotational speed. Table 6.4 also shows that ΔT tended to decrease with the increase of the conductive complex in the blends, which is expected as the torque levels also decreased in the same manner (refer to Table 6.2).

6.3 CONDUCTIVITY MEASUREMENTS.

As pointed out before, these experiments were carried out to investigate the behaviour of the conductivity with respect to the content of the conductive complex in the blends. At the same time, the results were meant to provide reference data with which compare the results from the measurements on the extruded blends in order to observe the effect of the processing history on their level of conductivity. This will be dealt with in chapter 7.

For the measurements, the prepared blends were compression moulded into flat plaques of about 1 mm thick using a high temperature constant thickness film maker (GRASEBY SPECAC). About 0.3 g of the blends were placed between the preheated

plates of the press. The moulding was performed at 120°C and at a pressure of about 25 x 10^3 N/m^2 for 5 min. Three plaques were produced for each blend. The volume conductivity for each blend was evaluated at room temperature on five to ten specimens cut at random from their respective plaques. Specimens about 2.5 mm long, 2.0 mm wide and 1.00 mm thick were tested. For the conductivity evaluations, the specimens' electrical resistance was measured using the same instrument (i.e., Keithley 614 electrometer), auxiliary equipment and method described in section 4.7. Assuming that the resistance readings were performed in an ohmic regime [179,181], the volume conductivity was calculated in accordance with the diagram shown in fig. 6.1 and using the following equation:

$$\sigma = \frac{l}{AR} = \frac{l}{abR} \quad \text{.....}Eq.\ 6.1,$$

where:

σ = specimen volume conductivity,

l = specimen length,

A = specimen cross sectional area,

R = measured volume resistance,

a = specimen width, and

b = specimen thickness.

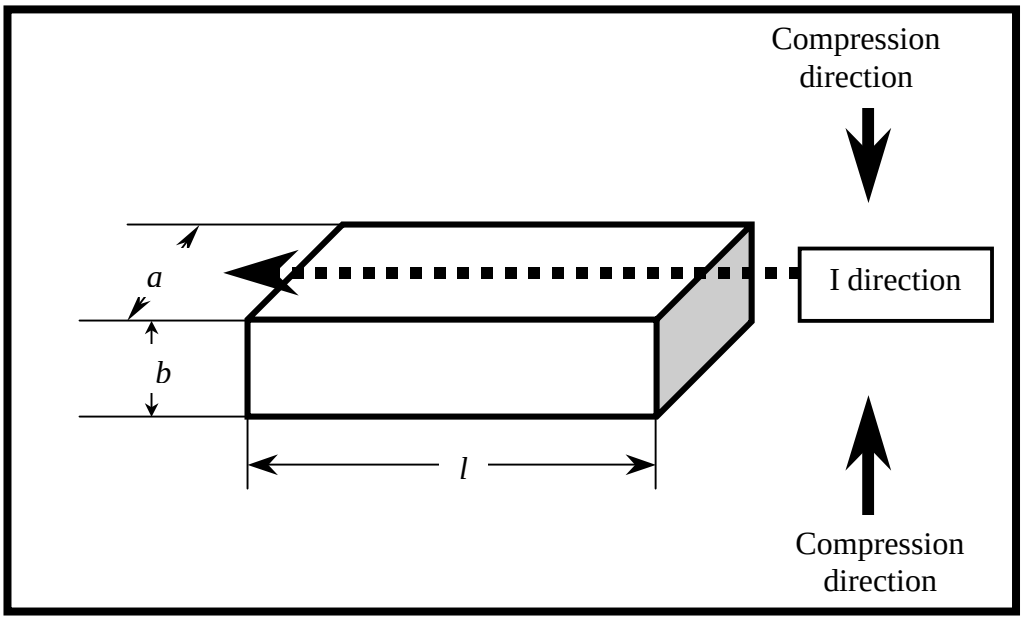

Figure 6.1. Diagram exemplifying the specimen dimensions. I = current, l = specimen length, a = specimen width, b = specimen thickness.

For the experiments, ten specimens of blends 5PANIPOL/SBS and 10PANIPOL/SBS were tested. However, seven specimens corresponding to blend 5PANIPOL/SBS showed resistance levels above 200 GΩ, which is the maximum reading achievable by the electrometer. The same occurred in two of the specimens of blend 10PANIPOL/SBS. Consequently, for the calculations, a value of 200 GΩ was taken as the estimated resistance of these specimens. On the other hand, for the blends 15PANIPOL/SBS and 20PANIPOL/SBS, eight specimens were evaluated which showed resistance levels within the range of resistances that the electrometer could measure. With respect to the blends 35PANIPOL/SBS and 50PANIPOL/SBS, only five specimens were tested as no significant scatter was observed in the results. The results of the calculations are presented in Table 6.5. The reader should therefore note that the average conductivity values presented for blends 5PANIPOL/SBS and 10PANIPOL/SBS are only approximations, and that the conductivity levels are overestimated, although not to a significant extent. On the other hand, the scatter observed in the conductivity levels corresponding to all the blends is most probably due to some degree of inhomogeneity in the composition of the blends.

Table 6.5. Results of the volume conductivity measurements on the PANIPOL™-SBS blends.

BLEND 5PANIPOL/SBS						
Specimen	***a* (mm)**	***b* (mm)**	***l* (mm)**	***R* (GΩ)**	**σ (S/cm)**	**Log σ**
1	0.75	1.90	1.41	74.8	1.32×10^{-10}	-9.88
2	1.09	1.33	1.06	84.2	8.68×10^{-11}	-10.06
3	0.80	1.45	1.42	81.4	1.50×10^{-10}	-9.82
4	1.12	1.29	1.90	> 200	$< 6.58 \times 10^{-11}$	-10.18
5	1.13	1.25	1.16	> 200	$< 4.11 \times 10^{-11}$	-10.39
6	1.23	1.31	1.16	> 200	$< 3.60 \times 10^{-11}$	-10.44
7	1.05	1.01	1.24	> 200	$< 5.85 \times 10^{-11}$	-10.23
8	0.74	0.95	1.04	> 200	$< 7.40 \times 10^{-11}$	-10.13
9	0.67	1.03	1.43	> 200	$< 1.04 \times 10^{-11}$	-10.98
10	1.02	0.98	1.44	> 200	$< 7.20 \times 10^{-11}$	-10.14
Average $\sigma = 7.27 \times 10^{-11}$ S/cm, Standard deviation of Log $\sigma = 0.33$						

Table 6.5. (Continued).

BLEND 10PANIPOL/SBS						
Specimen	***a* (mm)**	***b* (mm)**	***l* (mm)**	***R* (MΩ)**	**σ (S/cm)**	**Log σ**
1	1.14	1.97	2.03	50.0	1.81×10^{-7}	-6.74
2	1.16	1.95	2.00	24.1	3.67×10^{-7}	-6.44
3	1.18	1.81	2.44	0.398	2.87×10^{-5}	-4.54
4	1.14	1.29	2.18	13.6	1.10×10^{-6}	-5.96
5	1.12	2.30	2.22	$> 2 \times 10^{5}$	$< 4.31 \times 10^{-11}$	-10.37
6	1.12	1.28	2.46	$> 2 \times 10^{5}$	$< 8.58 \times 10^{-11}$	-10.07
7	1.17	1.40	1.77	100.5	1.10×10^{-7}	-6.96
8	1.15	1.19	1.57	9.63	1.19×10^{-6}	-5.93
9	1.16	1.11	1.75	4.3	3.16×10^{-6}	-5.50
10	0.77	1.06	1.19	85.5	1.71×10^{-7}	-6.77
Average $\sigma = 3.50 \times 10^{-6}$ S/cm, Standard deviation of Log $\sigma = 1.88$						
BLEND 15PANIPOL/SBS						
Specimen	***a* (mm)**	***b* (mm)**	***l* (mm)**	***R* (kΩ)**	**σ (S/cm)**	**Log σ**
1	1.48	2.01	2.14	1.04×10^{3}	6.92×10^{-6}	-5.16
2	1.42	2.03	2.26	133.1	5.89×10^{-5}	-4.23
3	1.31	1.95	2.13	415	2.01×10^{-5}	-4.70
4	1.46	1.89	2.08	67.1	1.12×10^{-4}	-3.95
5	1.49	1.91	2.19	121.6	6.33×10^{-5}	-4.20
6	1.01	1.44	2.49	2.91×10^{3}	5.88×10^{-6}	-5.23
7	1.57	2.00	2.11	92.0	7.30×10^{-5}	-4.14
8	1.06	1.52	2.22	35.8×10^{3}	3.85×10^{-7}	-6.42
Average $\sigma = 4.26 \times 10^{-5}$ S/cm, Standard deviation of Log $\sigma = 0.83$						
BLEND 20PANIPOL/SBS						
Specimen	***a* (mm)**	***b* (mm)**	***l* (mm)**	***R* (kΩ)**	**σ (S/cm)**	**Log σ**
1	0.90	2.06	2.78	103.0	1.46×10^{-4}	-3.84
2	1.05	1.89	2.87	73.4	1.97×10^{-4}	-3.71
3	0.90	1.94	2.35	171.4	7.85×10^{-5}	-4.11
4	1.02	1.94	2.34	50.0	2.37×10^{-4}	-3.63
5	0.95	1.95	2.23	18.3	6.58×10^{-4}	-3.18
6	1.00	1.89	1.93	538.0	1.90×10^{-5}	-4.72
7	1.03	2.04	2.12	40.6	2.49×10^{-4}	-3.60
8	1.00	2.11	2.26	111.4	9.62×10^{-5}	-4.02
Average $\sigma = 2.10 \times 10^{-4}$ S/cm, Standard deviation of Log $\sigma = 0.45$						

Table 6.5. (Continued).

BLEND 35PANIPOL/SBS						
Specimen	***a* (mm)**	***b* (mm)**	***l* (mm)**	***R* (kΩ)**	**σ (S/cm)**	**Log σ**
1	1.27	1.80	2.07	21.8	4.15 x 10^{-4}	-3.38
2	1.32	1.82	2.22	5.76	1.60 x 10^{-3}	-2.80
3	1.23	1.68	2.41	916.0	1.27 x 10^{-5}	-4.90
4	1.33	1.75	2.10	36.8	2.45 x 10^{-4}	-3.61
5	1.29	1.79	2.22	25.3	3.80 x 10^{-4}	-3.42
Average σ = 5.32 x 10^{-4} S/cm, Standard deviation of Log σ = 0.78						
BLEND 50PANIPOL/SBS						
Specimen	***a* (mm)**	***b* (mm)**	***l* (mm)**	***R* (kΩ)**	**σ (S/cm)**	**Log σ**
1	1.37	1.67	1.94	40.4	2.10 x10^{-4}	-3.68
2	1.38	1.63	2.12	5.35	1.76 x 10^{-3}	-2.76
3	1.40	1.54	2.03	78.2	1.20 x 10^{-4}	-3.92
4	1.40	1.56	2.13	9.21	1.06 x 10^{-3}	-2.98
5	1.35	1.64	2.36	16.29	6.54 x 10^{-4}	-3.18
Average σ = 7.61 x 10^{-4} S/cm, Standard deviation of Log σ = 0.49						

The average volume conductivity versus PANIPOL^{TM} 2 content in the blends is presented in figure 6.2 together with the rest of the experimental results. In the same way, for comparison purposes, the volume conductivity of the SBS (refer to section 3.3.1) and PANIPOL^{TM} 2 pellets (refer to section 4.7) is also respectively presented as 0 and 100 wt.% of PANIPOL^{TM} in the blends. In principle, the conductivity of both materials (SBS and PANIPOL pellets) should have been evaluated on specimens subjected to the same processing history to which the specimens of the blends were subjected. Although this is not strictly the case, the levels of conductivity presented for these two materials should not differ significantly from the levels that would be measured on specimens comparable to those of the blends.

Figure 6.2 shows that the conductivity of the PANIPOL^{TM}-SBS system does not present a well-defined insulator (or semiconductor)-conductor transition. However, the behaviour of conductivity with respect to composition is characteristic of a percolating system (refer to the relevant section in chapter 2) and is consistent with the data reported by other researchers on different polyaniline-based systems [11-13,20-23,29,56,57,62,66,162,187-190]. The experimental results presented in this section are

quantitatively analysed in more detail in chapter 8 where percolation and generalised effective media theories are used to estimate the percolation threshold, together with other parameters of interest.

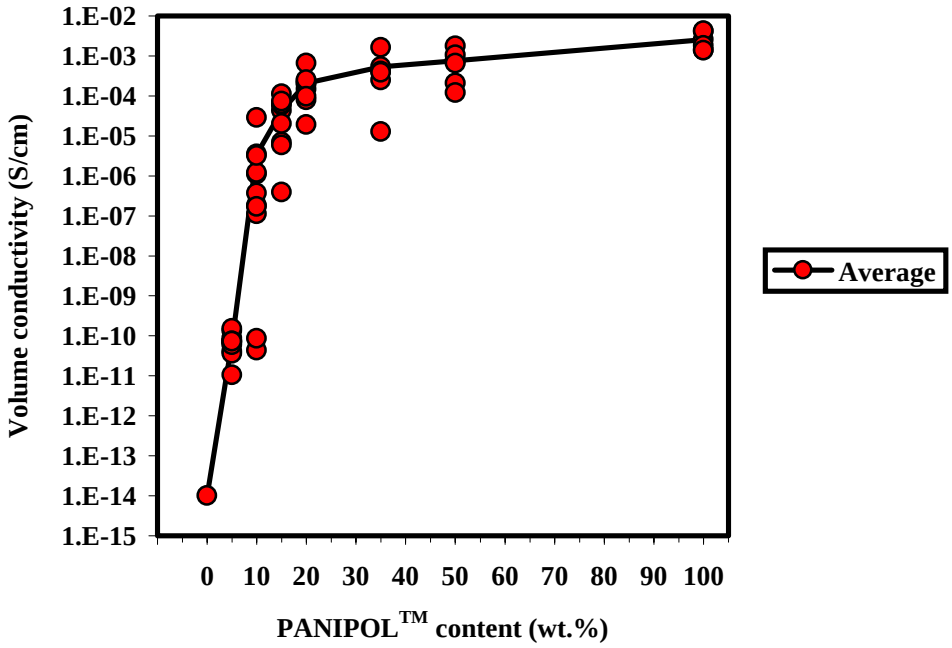

Figure 6.2. Volume conductivity of PANIPOL^{TM}2-SBS blends as a function of PANIPOL^{TM}2 weight percent.

The experimental results presented in fig. 6.2 suggest however, that the percolation threshold seems to occur at a PANIPOL^{TM} content of about 5 wt.% ($\sigma \sim 7 \times 10^{-11}$ S/cm). Additionally, the average conductivity of the blend with 10 wt.% of conductive complex (~ 4 x 10^{-6} S/cm) represents an abrupt increase of about eight orders of magnitude in the percolation region. Beyond this point, the conductivity level gradually increases with the increase of PANIPOL^{TM} content, reaching an average conductivity of ca. 2 x 10^{-4} S/cm for the blend with 20 wt.% of PANI complex. This level of conductivity is of the same order of magnitude to that observed for the blend with 50 wt.% of conductive complex (~ 8 x 10^{-4} S/cm). Moreover, these conductivity values are very close to that of the PANIPOL^{TM} pellets ($\sigma \sim 3 \times 10^{-3}$ S/cm) depicted in fig. 6.2 as 100 wt.% of PANIPOL^{TM}. As noted, the difference is less than one order of magnitude, which suggests that blending SBS with no more than 20 wt.% of PANIPOL^{TM}2 could produce an electrically conductive composite with a reasonably

good level of conductivity. On the other hand, the conductivity levels of all the PANIPOL^{TM}-SBS blends were generally within the typical range reported by Neste Oy Chemicals for PANIPOL^{TM}-based blends (i.e., 10^{-10}-10^{-1} S/cm) [71].

6.4 MORPHOLOGICAL ANALYSIS.

The microstructure responsible for the blends' conductance was elucidated following a combination of analysis techniques. Initially, morphological analysis was carried out on the fracture surface of cryogenically fractured specimens and on the surface of specimens subjected to an etching process. The analysis was performed by using scanning electron microscopy. The morphology of the blends was additionally studied by transmission electron microscopy (TEM). The details are presented in the following Sections.

6.4.1 SCANNING ELCTRON MICROSCOPY: FRACTURED SPECIMENS.

The analysis was performed with a JEOL JXA-840-A electron probe microanalyzer at 10 kV. The specimens studied were small rectangular bars cut from selected compression moulded blends. For comparison purposes, the morphology of a compression moulded specimen of SBS was also examined. As for other compression moulded specimens that will be referred to throughout the text, the compression moulding machine and parameters used are the same ones used in the preparation of the specimens for conductivity measurements (refer to section 6.3). Additional examination was performed on small bars cut from selected uncompressed blends. The specimens were fractured by immersion in liquid nitrogen. The fracture was achieved by bending the specimens, with the help of needle pliers, while they were into the liquid nitrogen and after 3 min of immersion (fig. 6.3). For the compression moulded specimens, the fracture was produced across their transverse section on which the examination was performed (refer to figs. 6.1 and 6.4). Specimens obtained from blends with 10, 20 and 50 wt.% of PANIPOL^{TM} were selected for analysis. These, together with the specimen of SBS, were gold coated for 4 min in an E5000 (Polaron Equipment Limited) SEM coating unit.

The SEM analysis showed that the specimens failed in a brittle manner, which is expected as they were fractured at a temperature well below their glass transition point (T_g), that is, at a temperature not higher than –195.8^{o}C, which is the nitrogen's boiling point [191] (note that the T_g of the doped PANI, PB and PS are around –20, –100 and 99°C, respectively).

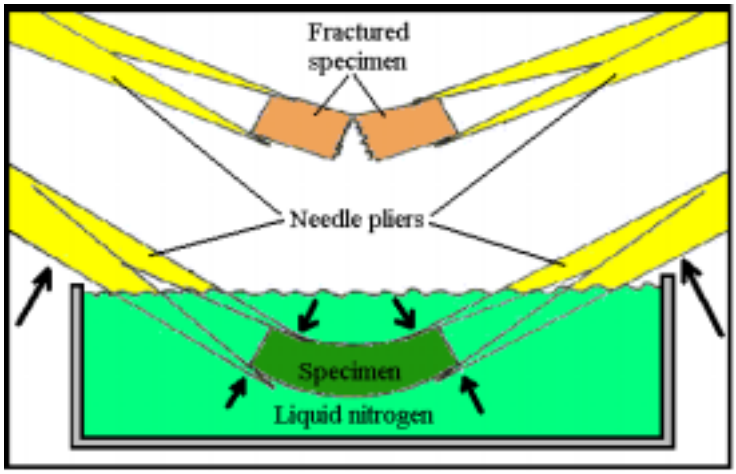

Figure 6.3. Schematic representation of the specimens' fracture. The arrows indicate the direction of the main bending forces applied on the specimens.

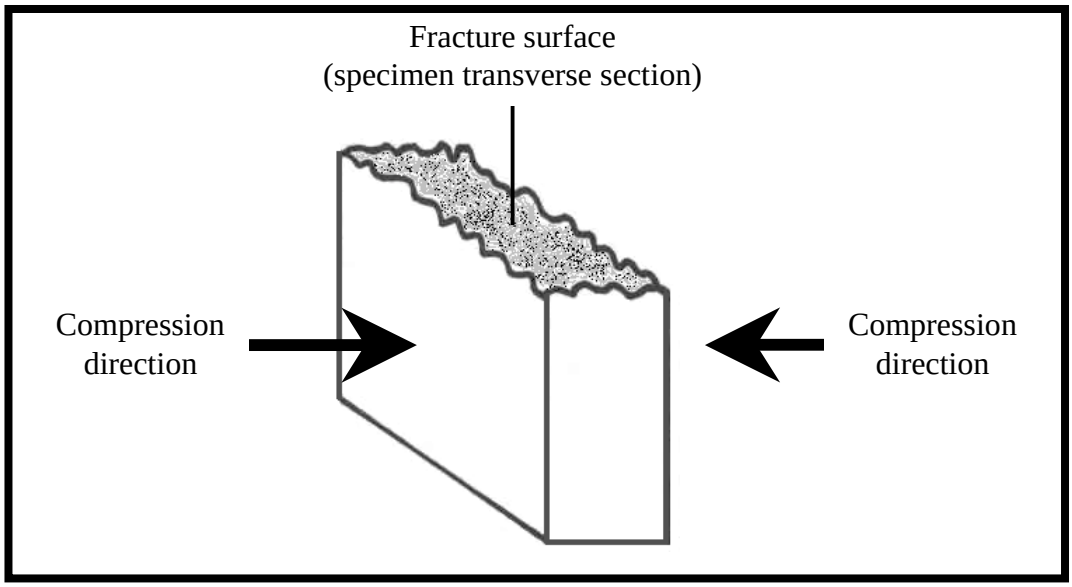

Figure 6.4. Schematic representation of the compression moulded specimens' fracture surface.

Some of the examined fracture surfaces did not provide any relevant morphological information, that is, the PANIPOL™ and SBS phases were not clearly identified. This was observed particularly in the uncompressed specimen of blends with 10 and 50 wt.% of conductive complex and in the compression moulded specimen of 10PANIPOL/SBS. However, the rest of the analysed fracture surfaces presented an interesting morphology well worthy of comment. For example, the fracture surface of the uncompressed specimen of blend 20PANIPOL/SBS (fig. 6.5) showed two types of morphologies that can be clearly identified, one rich of particle-like features dispersed in a continuous phase (e.g., the areas encircled in red in the figure) and another one free of these features (e.g. the areas encircled in yellow). These morphologies can be better observed in figure 6.5b, which corresponds to the same specimen but analysed at a higher magnification.

From figure 6.5b it can be observed that many of the features contained in the areas encircled in red appear to be globular-shaped particles. The morphology observed in these areas resemble to some extent the morphology observed in the powdered pellets of PANIPOL™ (refer to figures 4.34a, b and c in section 4.8.2) in which globular features, corresponding to the PANI particles, were also observed. It is therefore believed that the globular features observed in the aforementioned areas correspond to the polyaniline particles dispersed in the SBS matrix. On the other hand, the areas free of these features (e.g., the areas encircled in yellow) correspond to the SBS phase.

Figure 6.5b also indicates that the polyaniline domains are of about 2 μm in diameter or of a smaller size, which is in good agreement with the sizes observed by Davies et al. [66] in DBSA-doped PANI-SBS blends obtained by melt mixing in a BRABENDER® mixer. This reduction in size, with respect to the original size of the polyanilene particles observed in the powdered pellets (particles of up to about 7 μm in diameter were observed), is attributed to the high fracturing degree at which the original PANI particles were subjected. This, resulting from the high interaction level of the PANI phase with the SBS matrix during the mixing process.

With respect to the compression moulded specimen of blend 20PANIPOL/SBS, its fracture surface (fig. 6.6) showed a similar morphology to that observed in the uncompressed specimen. For example, note the spherical features dispersed all over the

fracture surface (some of them are indicated by red arrows). In fig. 6.6, the black arrows indicate the compression direction.

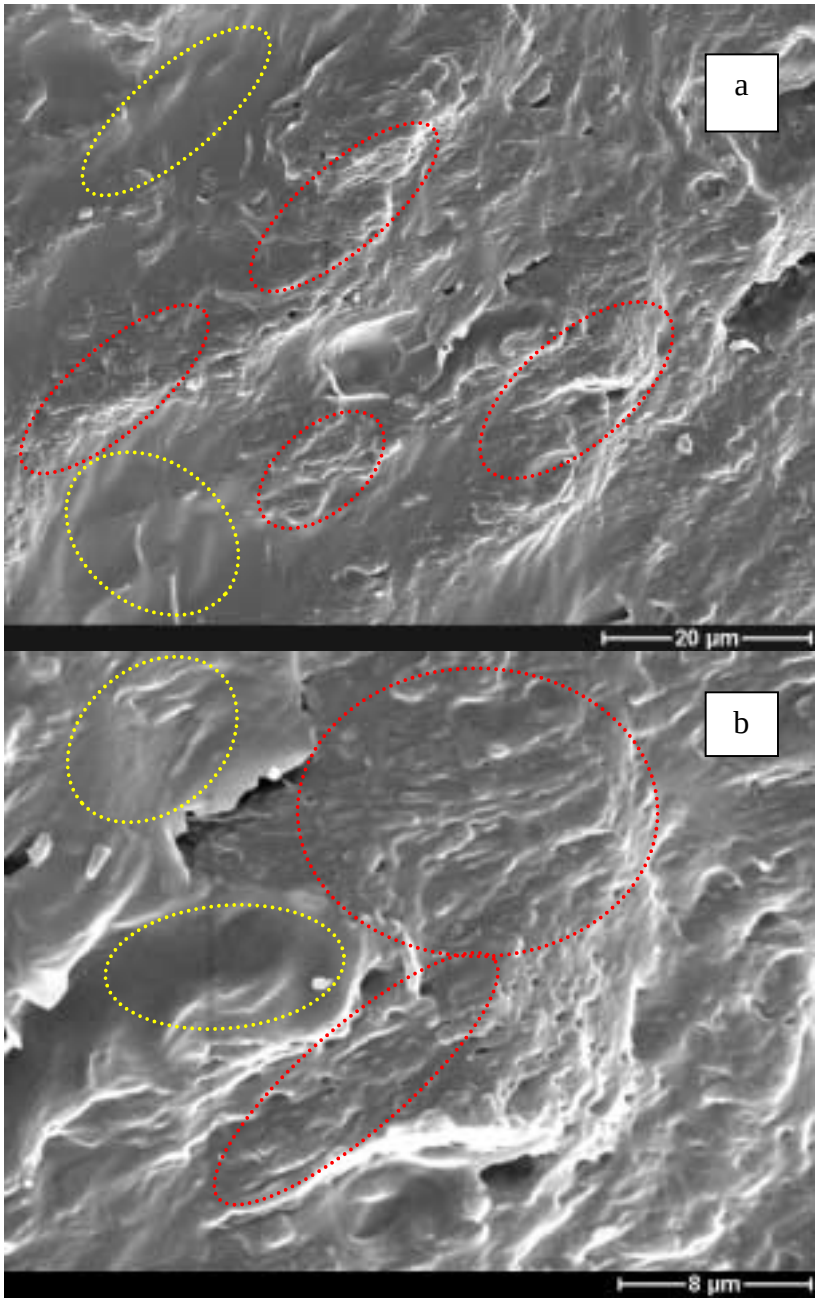

Figure 6.5. SEM micrographs of the fracture surface of a cryogenically fractured uncompressed specimen of 20PANIPOL/SBS analysed at different magnifications.

Again, it is believed that the spherical features observed in fig. 6.6 correspond to the PANI particles dispersed in the SBS matrix. This hypothesis is supported by comparing fig. 6.6 with fig. 6.7, which corresponds to the fracture surface of a

compression moulded specimen of SBS. As can be seen in fig. 6.7, similar plateau-like features to those observed in fig. 6.6 are observed in the fracture surface. However, in contrast with the morphology observed in fig. 6.6, the plateau-like features in fig. 6.7 are free of spherical features.

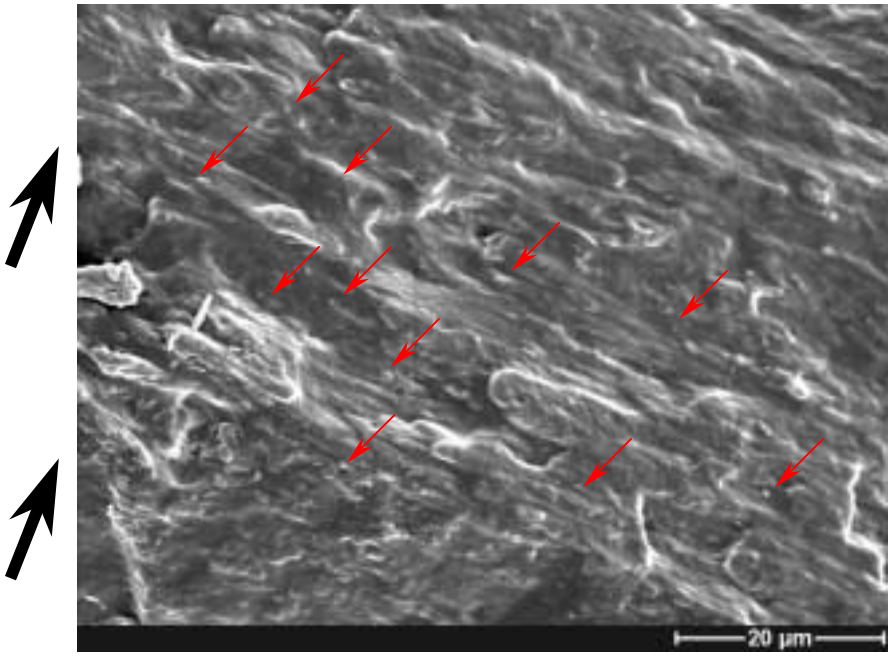

Figure 6.6. SEM micrograph of the fracture surface of a cryogenically fractured compression moulded specimen of 20PANIPOL/SBS. The arrows indicate the compression direction.

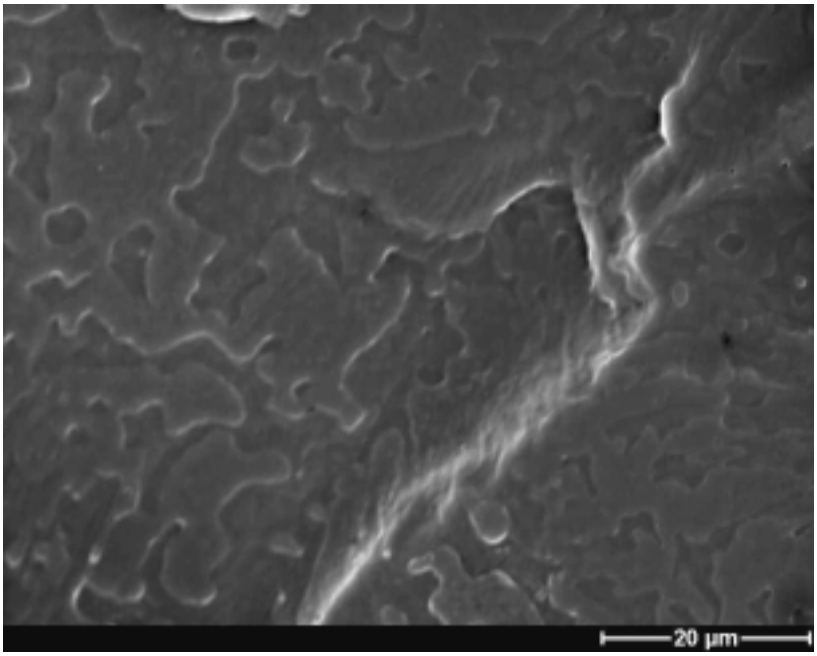

Figure 6.7. SEM micrograph of the fracture surface of a cryogenically fractured compression moulded specimen of SBS. The arrows indicate the compression direction.

It is interesting to note that fig. 6.6 also shows numerous elongated features aligned perpendicular to the compression direction that are absent in fig. 6.7. Therefore, it is possible that some of these features correspond to the edges of fractured layered structures of polyaniline, which were formed during the compression moulding process. It is very likely that these structures resulted from biaxial flow in which relatively large aggregates of PANI particles contracted on planes parallel to the compression forces and expanded (flowed) in all directions on planes perpendicular to the compression direction.

The morphologies observed on the fracture surface of the specimens of blend 20PANIPOL/SBS, are in good agreement with those observed by Zilberman et al. [21,23] in different cryogenically fractured systems based on DBSA-doped PANI.

The concept about the formation of layered structures of polyaniline in the compression moulded specimens is reinforced by the morphologies observed on the fracture surface of the compression moulded specimen of blend 50PANIPOL/SBS (fig. 6.8). As can be seen, fig. 6.8 shows many elongated features aligned perpendicular to the compression direction, which also display a considerable degree of continuity and uniformity. The absence of these features on the fracture surface of the SBS specimen (figs. 6.7 and 6.9), analysed at comparable magnifications to those used in the analysis of the specimen of blend 50PANIPOL/SBS, suggests again that they correspond to the edges of fractured layers of polyaniline that were formed during the compression moulding process.

Figure 6.8 also suggests that the concentration of elongated features as well as their degree of continuity and uniformity seem to be higher in the specimen of blend 50PANIPOL/SBS than in that of blend 20PANIPOL/SBS. This is expected as the former blend has a higher content of PANIPOL^{TM}, which also explains the higher level of conductivity in their specimens. On the other hand, figure 6.8b indicates that the layers of PANI should be about 2 μm thick or even thinner. However, a better estimate of their thickness will be provided by means of the transmission electron micrographs (section 6.4.3).

To this point, the morphological information obtained from the SEM micrographs presented in this section indicates that the conduction of electricity occurs through

continuous paths of polyaniline, in the form of layered structures, formed within the SBS matrix in the compression moulded specimens. However, the morphological analysis presented in the following sections will verify this hypothesis.

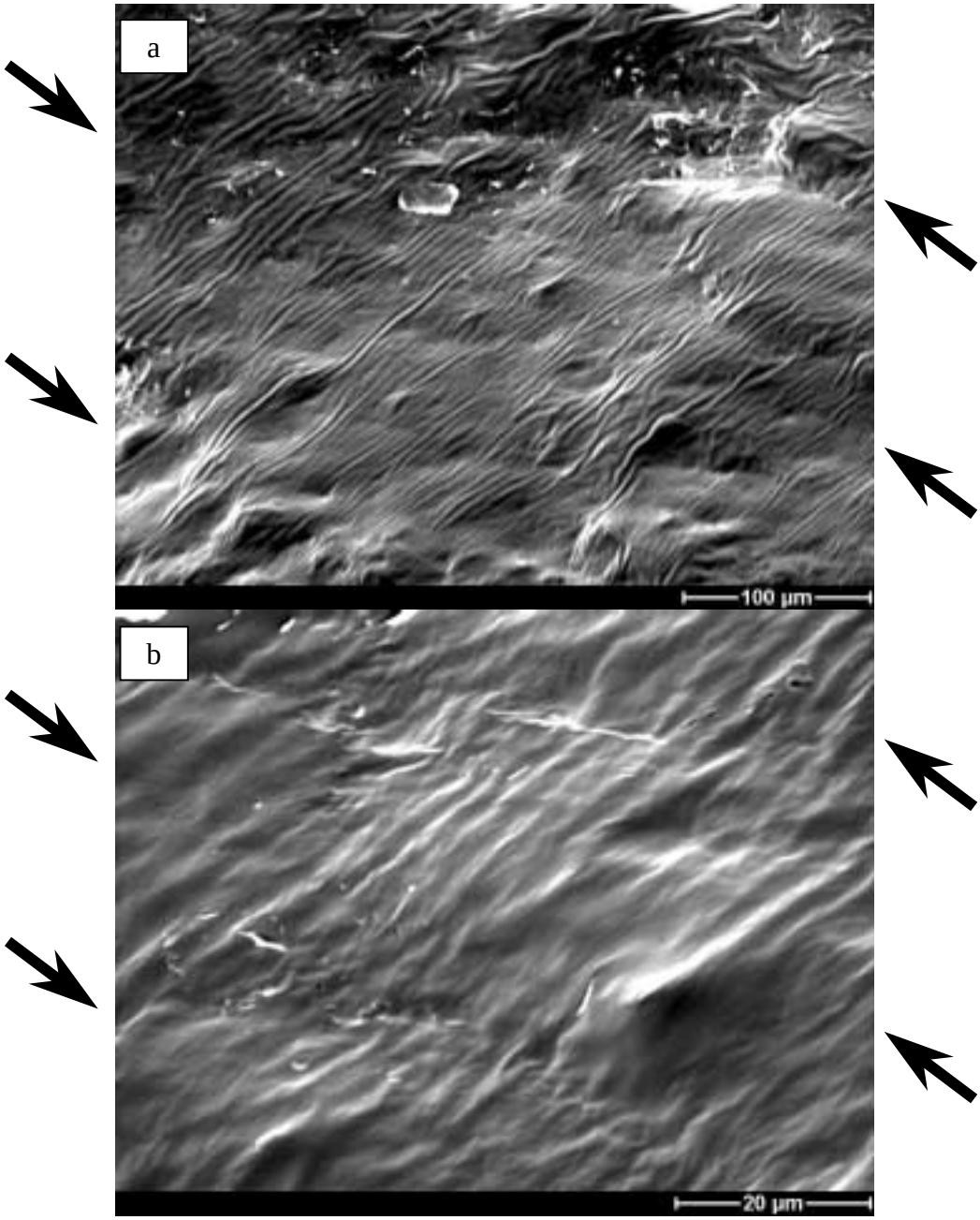

Figure 6.8. SEM micrographs of the fracture surface of a cryogenically fractured compression moulded specimen of 50PANIPOL/SBS analysed at different magnifications. The arrows indicate the compression direction.

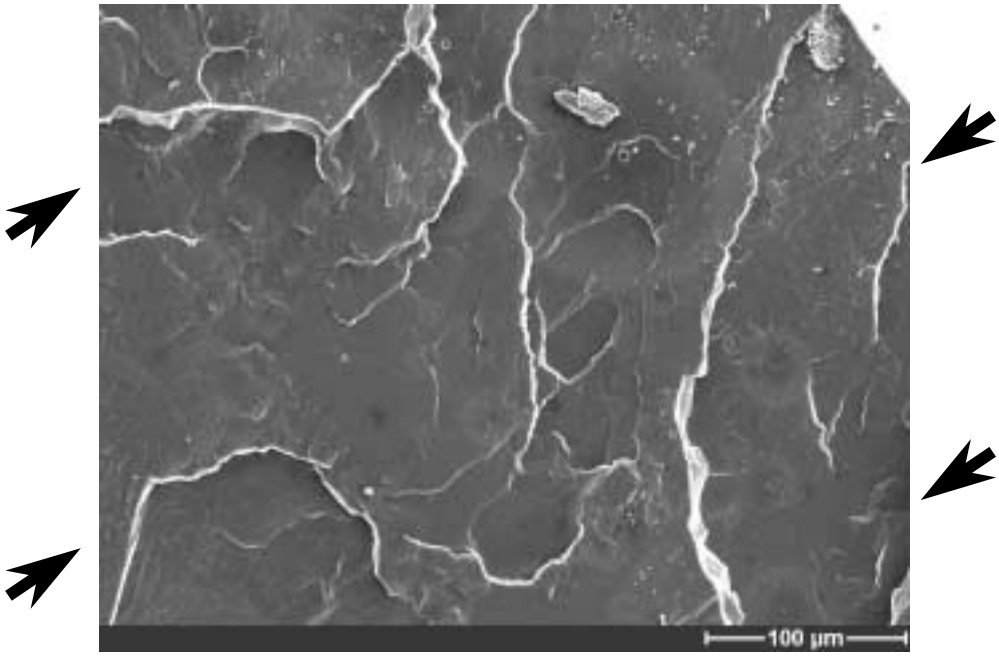

Figure 6.9. SEM micrograph of the fracture surface of a cryogenically fractured compression moulded specimen of SBS (as fig. 6.7 but analysed at a lower magnification). The arrows indicate the compression direction.

6.4.2 SCANNING ELCTRON MICROSCOPY: ETCHED SPECIMENS.

The analysis was carried out using the SEM instrument described in the previous section. Similarly, the morphology of the transverse section of small rectangular bars, cut from selected compression moulded blends, was analysed. The morphology of the transverse section of a compression moulded specimen of SBS was also examined for comparison purposes. Specimens obtained from blends 10PANIPOL/SBS, 20PANIPOL/SBS and 50PANIPOL/SBS were selected for analysis. The purpose of etching the specimens was to remove selectively one of the phases from their surface, leaving the other one (ideally the PANI phase) exposed for examination. Accordingly, the specimens were immersed, for 72 hrs, in a mixture of chromic and phosphoric acids comprising 100 ml of sulphuric acid (H_2SO_4), 30 ml of phosphoric acid (H_3PO_4), 5 g of chromium oxide (CrO_3) and 30 ml of distilled water. All the chemicals, of 99 % chemical purity, were provided by Aldrich Labs. Only one ml of mixture was used in the preparation of the specimens. After immersion, the specimens were washed with an excess of distilled water and, afterwards, dried overnight in a vacuum oven at 40°C. Subsequently, the specimens were kept in a desiccator to await further analysis. For the

analysis, the specimens were gold coated for 4 min in an E5000 (Polaron Equipment Limited) SEM coating unit.

The etching solution used is a powerful oxidising agent commonly used in the preparation of specimens of toughened plastics for morphological characterisation [192]. This, which selectively attacks the unsaturated PB phase and has little effect upon the PS phase, was originally intended to remove part of the SBS matrix from the surface of the specimens, leaving the polyaniline phase exposed. However, it was realized that doped PANI is also attacked (dissolved) by strong acids like H_2SO_4 [48,58]. Therefore, the etching agent would not only remove the SBS phase, but also the polyaniline phase, which would impede the interpretation of the morphology observed on the surface of the specimens. This problem was partially overcome by analysing the degree of susceptibility of the polyaniline and SBS to attack by the etching agent. For this, an experiment was performed in which PANIPOL^{TM} and SBS pellets, of similar surface areas, were respectively subjected to the same etching process to which the compression moulded specimens were subjected. The analysis was performed on five pellets of each material. After the immersion time elapsed, each pellet was washed with distilled water, dried overnight in a vacuum oven at 40°C, and afterwards, kept in a desiccator to await further analysis. The pellets were weighed and it was found that the average weight loss in the PANIPOL pellets was 27 %. In contrast, the average weight loss in the SBS pellets was only 1.35 %. Assuming that the surface areas of the PANIPOL and SBS pellets were the same, the results suggest that about 20 times more PANIPOL than SBS was lost due to the action of the etching agent. This suggests that the PANIPOL phase is more susceptible to attack, by the etching solution, than the SBS phase. Therefore, in principle, the PANIPOL phase would be mostly removed from the surface of the compression moulded specimens, leaving the SBS phase exposed. In other words, what would be mostly observed on the surface of the specimens would be the “footprints” of the PANI phase that was washed away, by the etching solution, from the SBS matrix.

During the analysis, some marks were observed on the transverse section of the compression moulded specimen of SBS. Therefore, it is possible that some of the marks observed on the surface of the compression moulded blends do not necessarily correspond to regions depleted of polyaniline, but to gaps (or voids) opened by the etching agent on the less dense areas of the SBS matrix, which in turn may have

resulted from an uneven compression moulding process. It is also possible that these voids originated because of an irregular etching process.

An example of what has been mentioned before can be seen in figure 6.10, which corresponds to the compression moulded specimen of SBS.

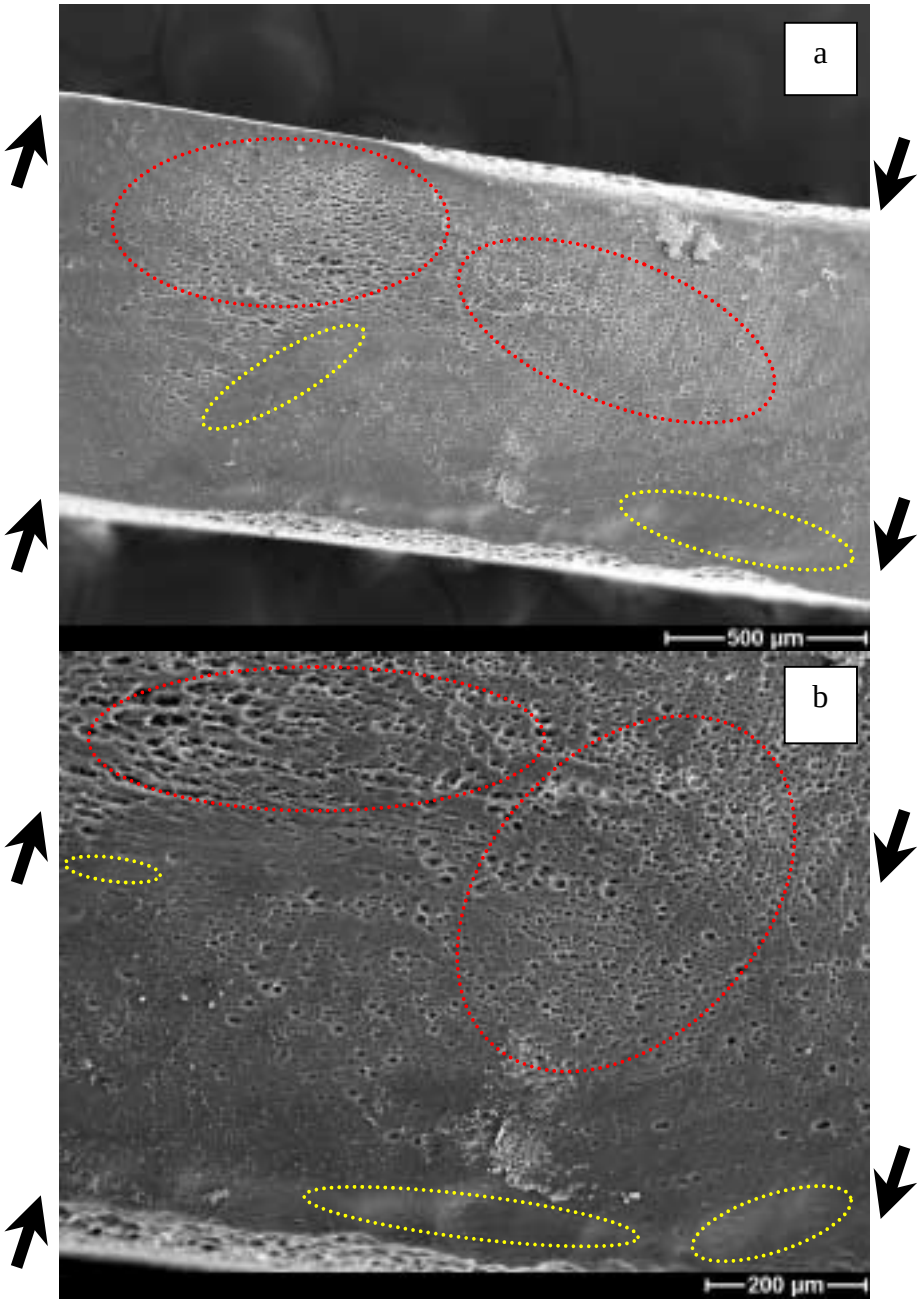

Figure 6.10. SEM micrographs of the transverse section of an etched specimen of compression moulded SBS analysed at different magnifications.

As in all the micrographs that have been, and will be presented in this chapter, the arrows in fig. 6.10 indicate the compression direction unless otherwise stated. As can be seen in fig. 6.10, some areas of the specimen's surface present a porous appearance (e.g. the areas encircled in red). On the other hand, a different morphology is observed in other areas (encircled in yellow) in which the surface of the specimen looks smoother, which is the type of morphology expected in etched specimens of SBS observed at these magnifications. Figure 6.10 also shows some lines (parallel or at certain angles to the compression direction), which are cutting artefacts. All this, as the reader may have already realized, creates some uncertainty about the interpretation of the morphologies observed in the specimens of the compression moulded blends. Nevertheless, some interesting structures were observed on the surface of the specimens, whose interpretation was assisted by the microstructure observed in the cryogenically fractured specimens previously commented on in section 6.4.1.

The morphology observed in the specimen of blend 10PANIPOL/SBS is presented in fig. 6.11. As can be seen, a similar porous surface to that observed in figs. 6.10a and b is evident in figs. 6.11a and b (note that the magnifications are comparable). However, differing from fig. 6.10, the latter two figures show a morphology in which very narrow, highly elongated cavities are most abundant. Additionally, these features, contrasting with those observed in fig. 6.10, and better observed in figs. 6.11c and d (one of them encircled in red), appear to have a higher degree of continuity and uniformity. Moreover, they also seem to be more aligned perpendicular to the compression direction than those observed in fig. 6.10. It is believed that the elongated cavities observed in fig. 6.11 (which are about 2 μm thick or thinner) mainly correspond to regions on the surface of the specimen in which the polyaniline phase was originally present and that was dissolved by the etching solution. As the cavities are highly aligned normal to the compression direction, this suggests again that, during compression, the polyaniline phase is arranged into a layered structure, within the SBS phase, parallel to the plates of the pressing instrument. Figure 6.11 also shows the presence of some circular (or shapeless) cavities (e.g., those indicated by yellow arrows), which perhaps correspond to regions depleted of small polyaniline clusters that were not deformed (elongated) during compression. It is also possible that these features correspond to cavities made on the SBS matrix by the etching agent.

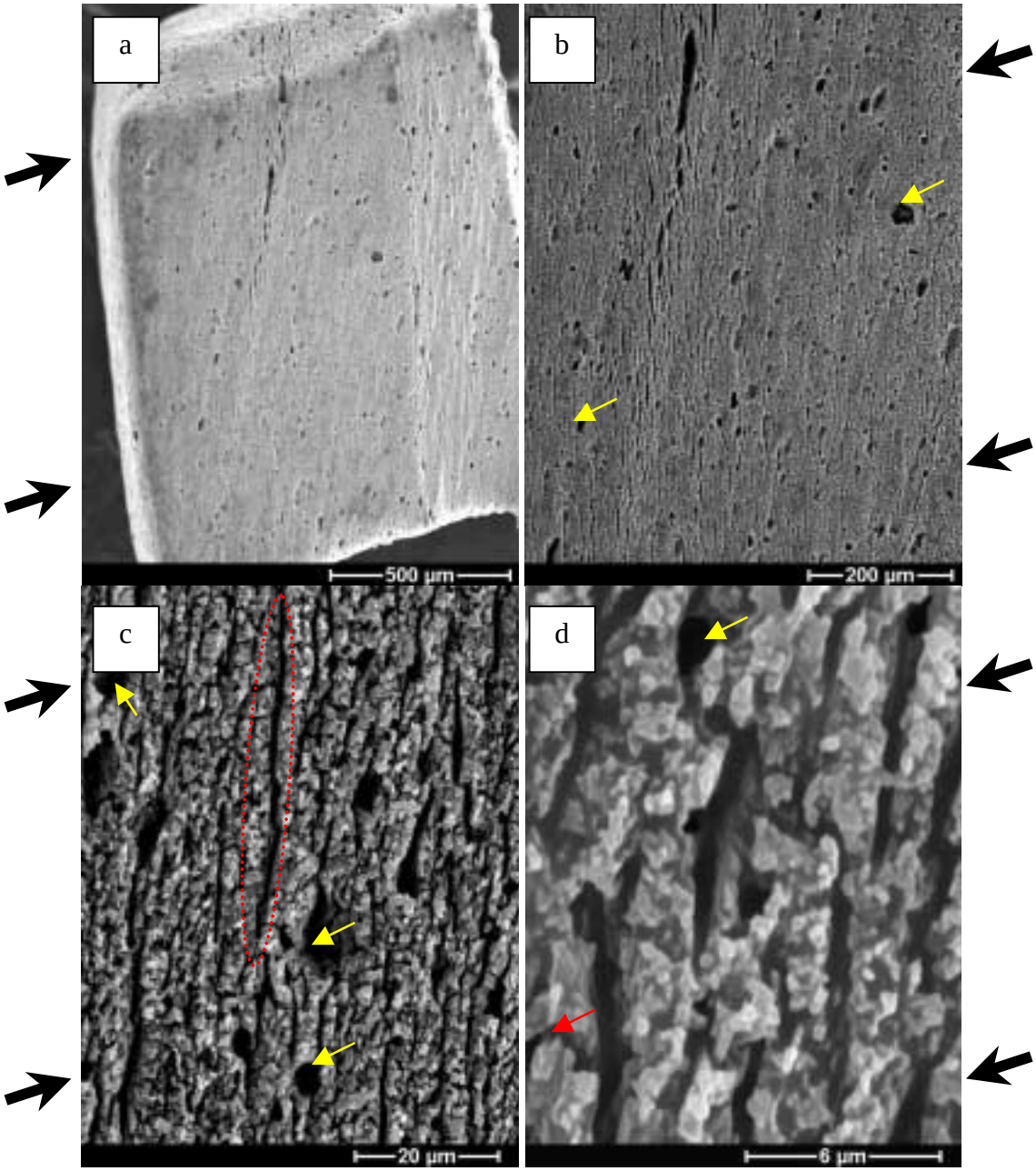

Figure 6.11. SEM micrographs of the transverse section of an etched specimen of the compression moulded blend 10PANIPOL/SBS analysed at different magnifications.

It is interesting to notice that figs. 6.11c and d also display numerous path-like cavities interconnecting the elongated voids (e.g., that one indicated by the red arrow). Whether these interconnecting cavities correspond to regions that were originally filled with polyaniline is difficult to establish through these micrographs. This will be verified by means of the TEM micrographs presented in the next section. Regardless of this, and

as has been noticed, the morphology observed in fig. 6.11 is consistent with that observed in the cryogenically fractured specimens.

With respect to the specimen of blend 20PANIPOL/SBS (fig. 6.12), a morphology of cavities of different sizes and shapes is observed. For example, note that most of the cavities contained in the areas encircled in yellow are smaller than those contained in the areas encircled in red. Moreover, the holes observed in the latter areas are highly elongated and aligned perpendicular to the compression direction. On the other hand, it is worthy of note that the elongated features contained in the areas encircled in red are wider than those observed on the surface of the specimen of blend 10PANIPOL/SBS (compare figs. 6.11b and 6.12b). Assuming that these features correspond to regions that were originally filled with polyaniline, the observed morphology would be expected as the specimen of blend 20PANIPOL/SBS has a higher content of conductive complex. However, for the reasons already explained, it is difficult to establish through these micrographs whether the observed cavities on the whole surface of the specimen correspond to depleted regions of PANI or to openings made on the SBS matrix by the etching solution.

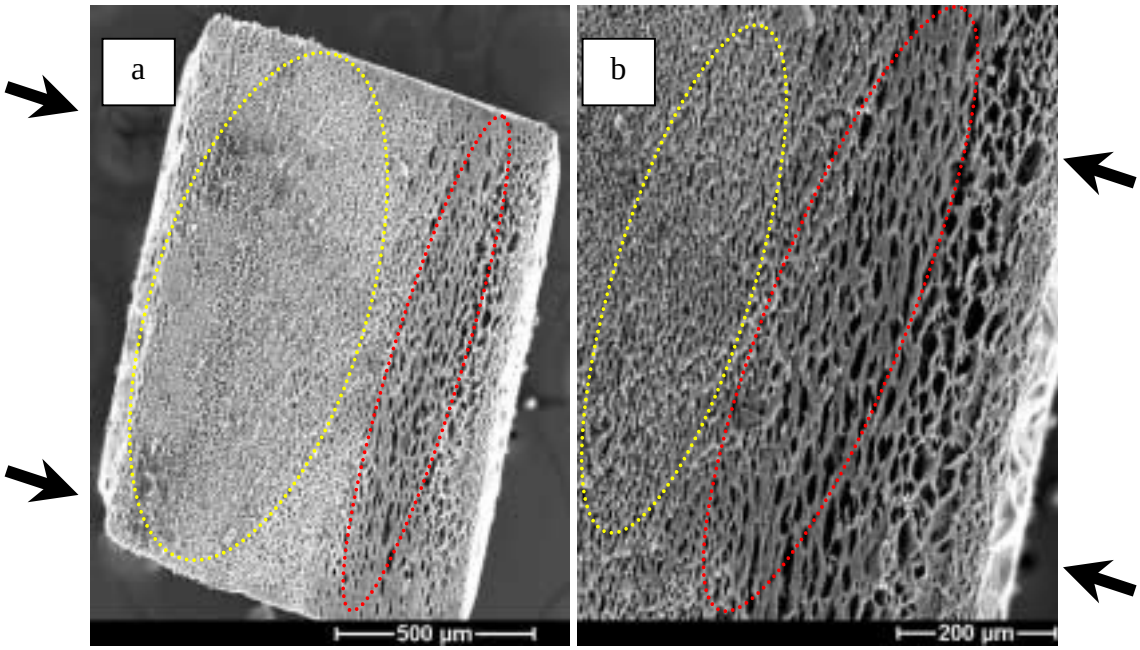

Figure 6.12. SEM micrographs of the transverse section of an etched specimen of the compression moulded blend 20PANIPOL/SBS analysed at different magnifications.

Regarding the specimen of blend 50PANIPOL/SBS (fig. 6.13), a large number of elongated cavities aligned perpendicular to the compression direction was found. Since these type of cavities are absent on the transverse section of the compression moulded specimen of SBS, this suggests once again that they correspond to depleted regions of polyaniline, which was originally on the surface of the specimen and that was dissolved by the mixture of chromic and phosphoric acids.

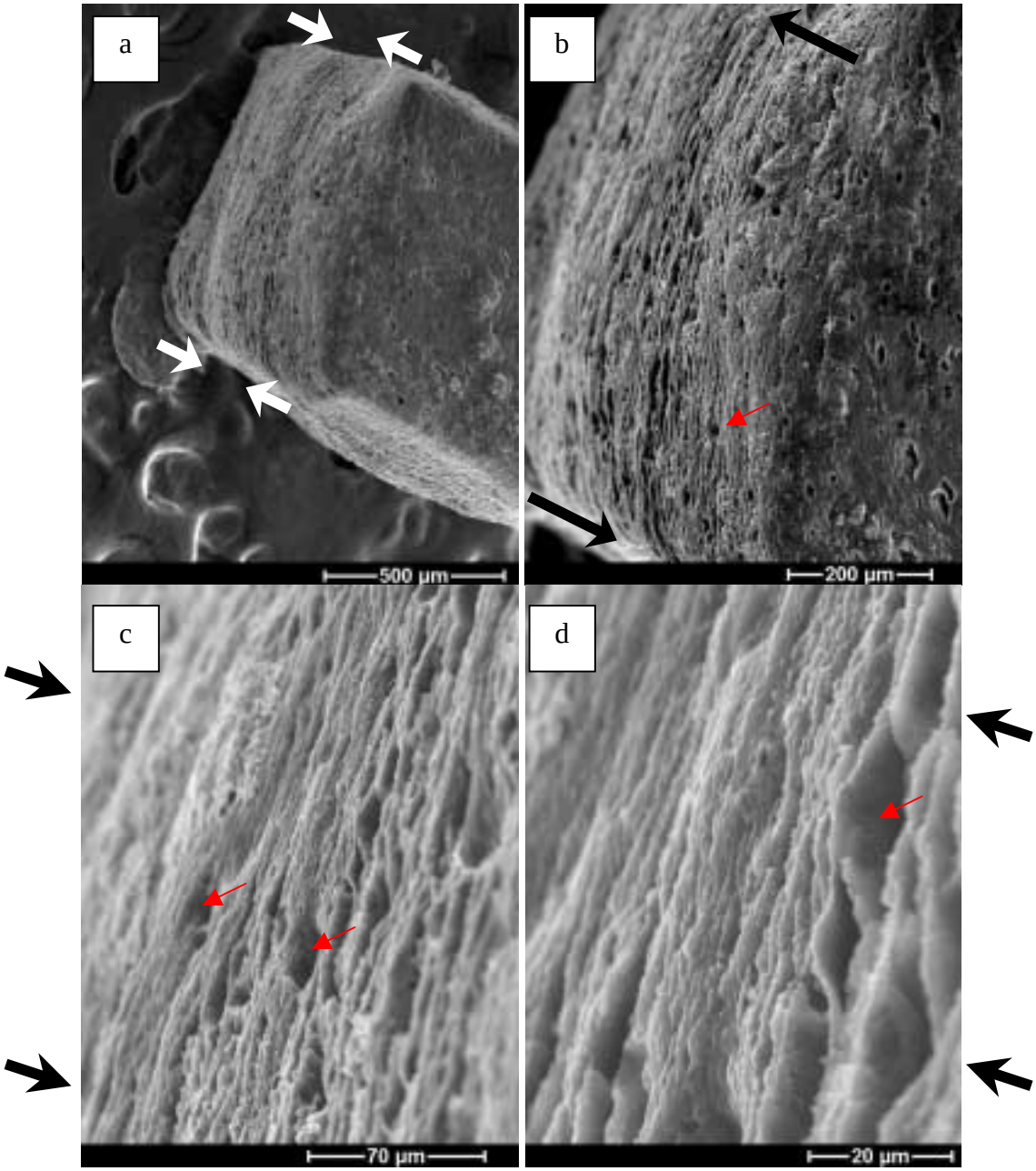

Figure 6.13. SEM micrographs of the transverse section of an etched specimen of the compression moulded blend 50PANIPOL/SBS analysed at different magnifications.

The absence of the elongated cavities, aligned perpendicular to the compression direction, on the transverse section of the specimen of SBS is better observed in figure 6.14, which is a micrograph of the same specimen shown in fig. 6.10 but viewed at a different angle, and analysed at the same magnification to that used for the analysis of the specimen of blend 50PANIPOL/SBS (fig. 6.13a).

Figure 6.13 also shows some shapeless (almost circular) cavities placed in between the elongated cavities, which may correspond to regions originally filled with polyaniline clusters that were not elongated during compression. These cavities are indicated in the figure by red arrows (the white and black arrows indicate the compression direction). As can be seen, the morphology observed on the transverse section of the specimen of blend 50PANIPOL/SBS is consistent with that observed on the transverse section of the cryogenically fractured specimen (fig. 6.8). This supports, yet again, the concept about the formation of layered structures of polyaniline during compression.

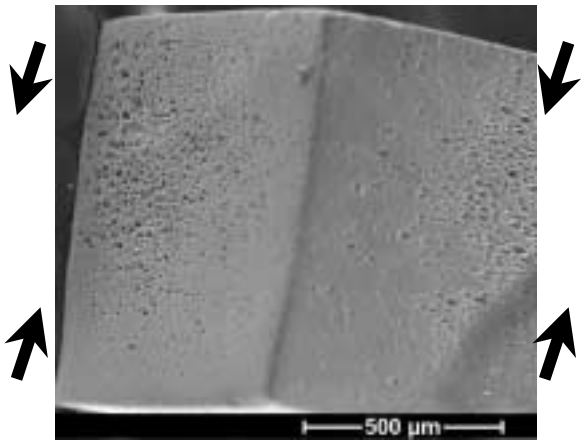

Figure 6.14. SEM micrograph of the transverse section of an etched specimen of compression moulded SBS (as fig. 6.10a but viewed at a different angle).

6.4.3 TRANSMISSION ELECTRON MICROSCOPY.

The morphology of the compression moulded blends was analysed in more detail with a JEOL 2000 FX transmission electron microscope using an accelerating voltage of 100 kV. As in the morphological analyses previously described in this chapter, the TEM analysis was carried out on the transverse section of specimens cut from selected compression moulded blends. The sections for analysis were obtained by cryo-

ultramicrotomy using a Reichert ultramicrotome (type 701701), fitted with a glass knife, and liquid nitrogen vapour to lower the temperature of the specimens. The specimens were embedded in a special epoxy resin such that a flat surface was exposed for cutting. Once the resin hardened, thin sections of about 200 nm thick were obtained for examination. The direction of sectioning was parallel to the compression direction. Specimens obtained from blends 5PANIPOL/SBS, 20PANIPOL/SBS and 50PANIPOL/SBS were selected for analysis.

The morphology observed in the specimen of blend 5PANIPOL/SBS is presented in fig. 6.15. As in the other micrographs that will be presented in this section, the darker features in fig. 6.15 correspond to the PANI phase, whereas the pale background correspond to the SBS phase. Some of the figures also show some whitish features such as small dots and lines (e.g., those ones encircled in red). These correspond to imperfections on the negatives that were printed during the production of the micrographs.

As can be seen, fig. 6.15 shows numerous well-defined elongated domains of polyaniline aligned perpendicular to the compression direction that should correspond to the cross section of layered structures of PANI, which were formed during the compression moulding process. From the figure, it can be noticed that these structures are about 0.08 μm thick (80 nm) or even thinner. Figure 6.15 also reveals the presence of a large number of discrete spot-like domains of PANI scattered all over the specimen's transverse section.

With respect to the specimen of blend 20PANIPOL/SBS, its morphology is presented in figures 6.16 and 6.17. As in other micrographs presented in this section, the areas encircled in yellow in fig. 6.16 correspond to regions of the sectioned specimen that were damaged by the electron beam during the analysis. As can be noticed, the specimen of blend 20PANIPOL/SBS exhibits many more polyaniline domains than that of blend 5PANIPOL/SBS. This is expected as the former specimen has a higher content of PANIPOL. On the other hand, although isolated domains of PANI are more abundant in fig. 6.16, the presence of elongated features is also evident. This is better observed in fig. 6.17, which shows that these features are highly aligned perpendicular to the compression direction. Figure 6.17 also suggests that some of the polyaniline layers

presumably present in the specimen of blend 20PANIPOL/SBS should be thicker than those present in the specimen of blend 5PANIPOL/SBS. For example, note that elongated feature, about 0.5 μm thick (500 nm), indicated by the red arrow in fig. 6.17.

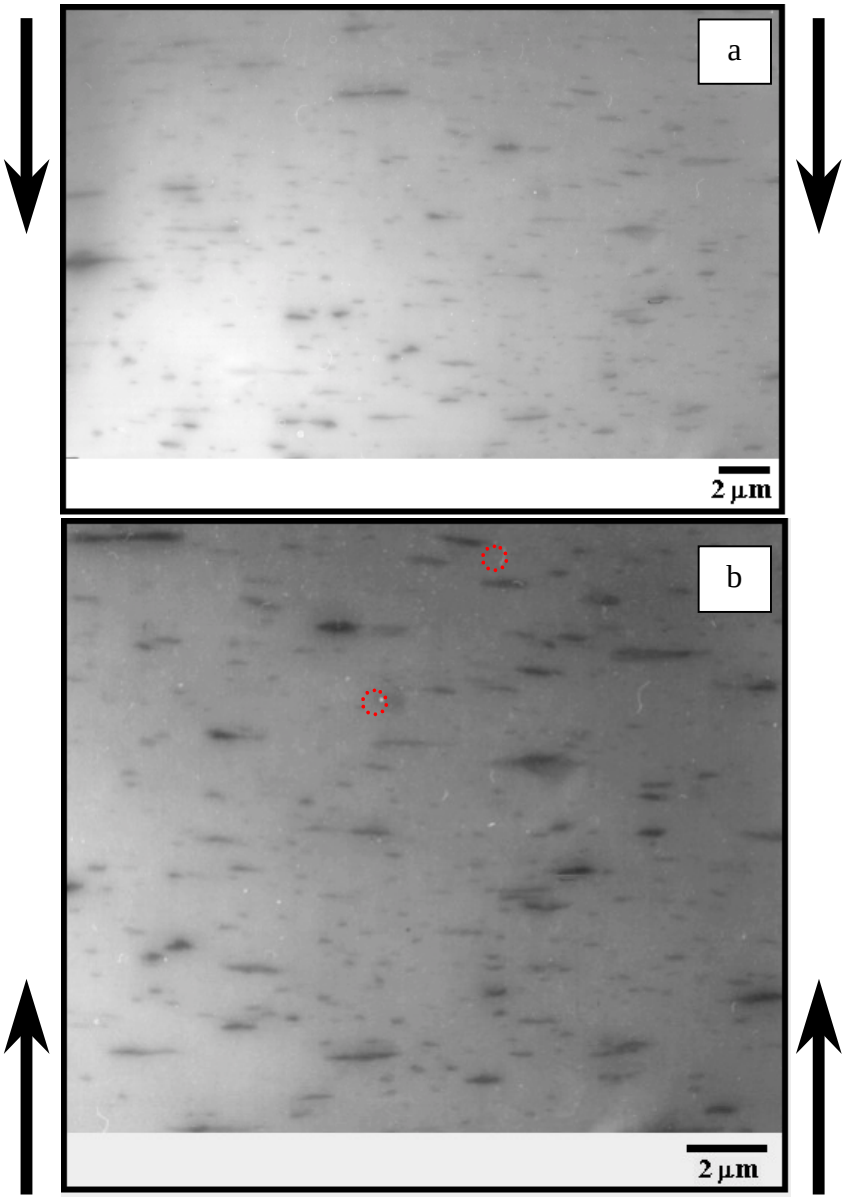

Figure 6.15. TEM micrographs of the transverse section of compression moulded blend 5PANIPOL/SBS analysed at different magnifications.

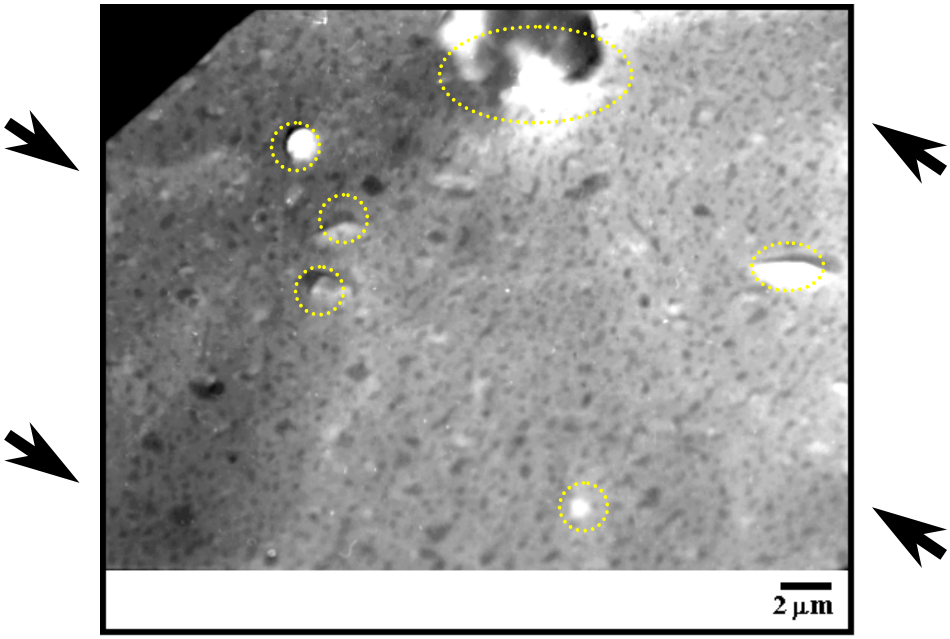

Figure 6.16. TEM micrograph of the transverse section of compression moulded blend 20PANIPOL/SBS.

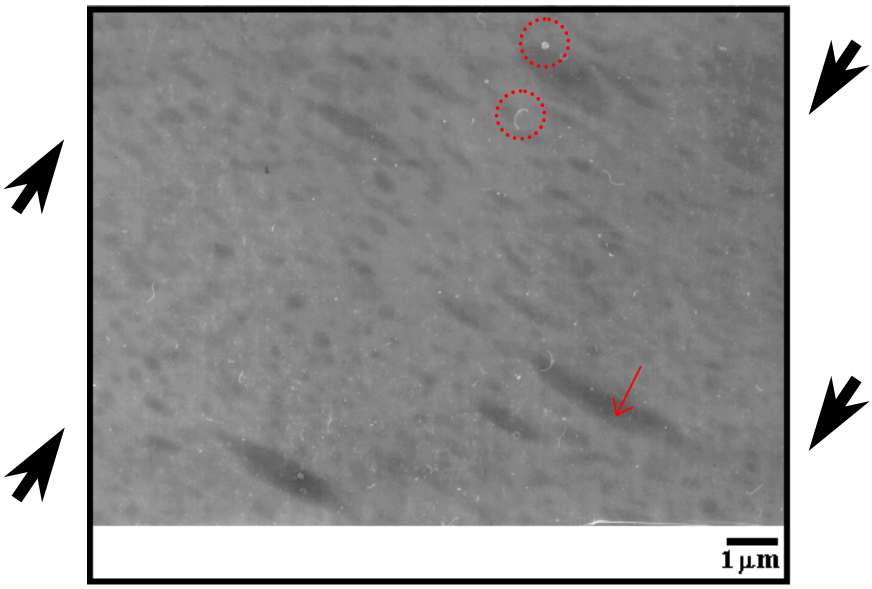

Figure 6.17. As fig. 6.16, but analysed at a higher magnification.

The formation of polyaniline layers during the compression moulding process was also evinced in the specimen of blend 50PANIPOL/SBS (figs. 6.18 and 6.19). As can be seen, this specimen not only exhibited numerous elongated domains of PANI, but also a higher content of these than in the specimens of the previous blends. Again, this is expected as blend 50PANIPOL/SBS has the highest content of conductive complex.

Figs. 6.18 and 6.19 also show that, although the elongated domains of PANI are not perfectly aligned perpendicular to the compression direction, they display a high degree of continuity. Moreover, they appear to be interconnected by numerous elongated domains of PANI, not necessarily aligned perpendicular to the compression direction. For instance, note the features indicated by the red arrows in the micrographs. Whether these features also correspond to the cross sections of layered structures of polyaniline, randomly oriented within the SBS matrix, is difficult to establish. Another possibility is that these features correspond to interconnecting PANI paths made within the insulating matrix during the compression moulding process. Irrespective of this, fig. 6.19a suggests a thickness of up to about 0.125 μm (125 nm) for the polyaniline layers present in the specimen in question.

It is interesting to notice that the specimen of blend 50PANIPOL/SBS also displays many discrete domains of PANI that seem to be connected to the elongated ones. Some of these features, similar to those found in the previous blends, are indicated in the figures by yellow arrows.

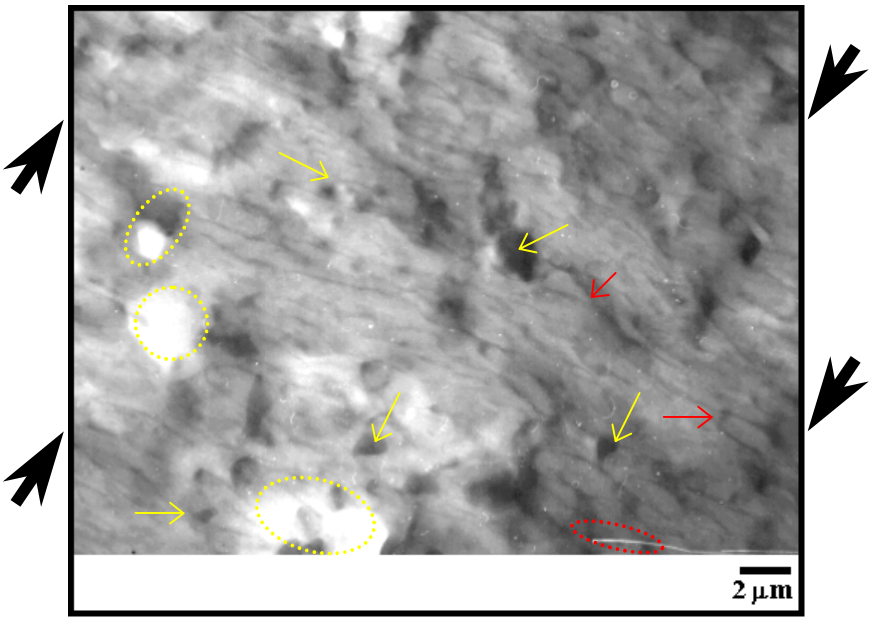

Figure 6.18. TEM micrograph of the transverse section of compression moulded blend 50PANIPOL/SBS.

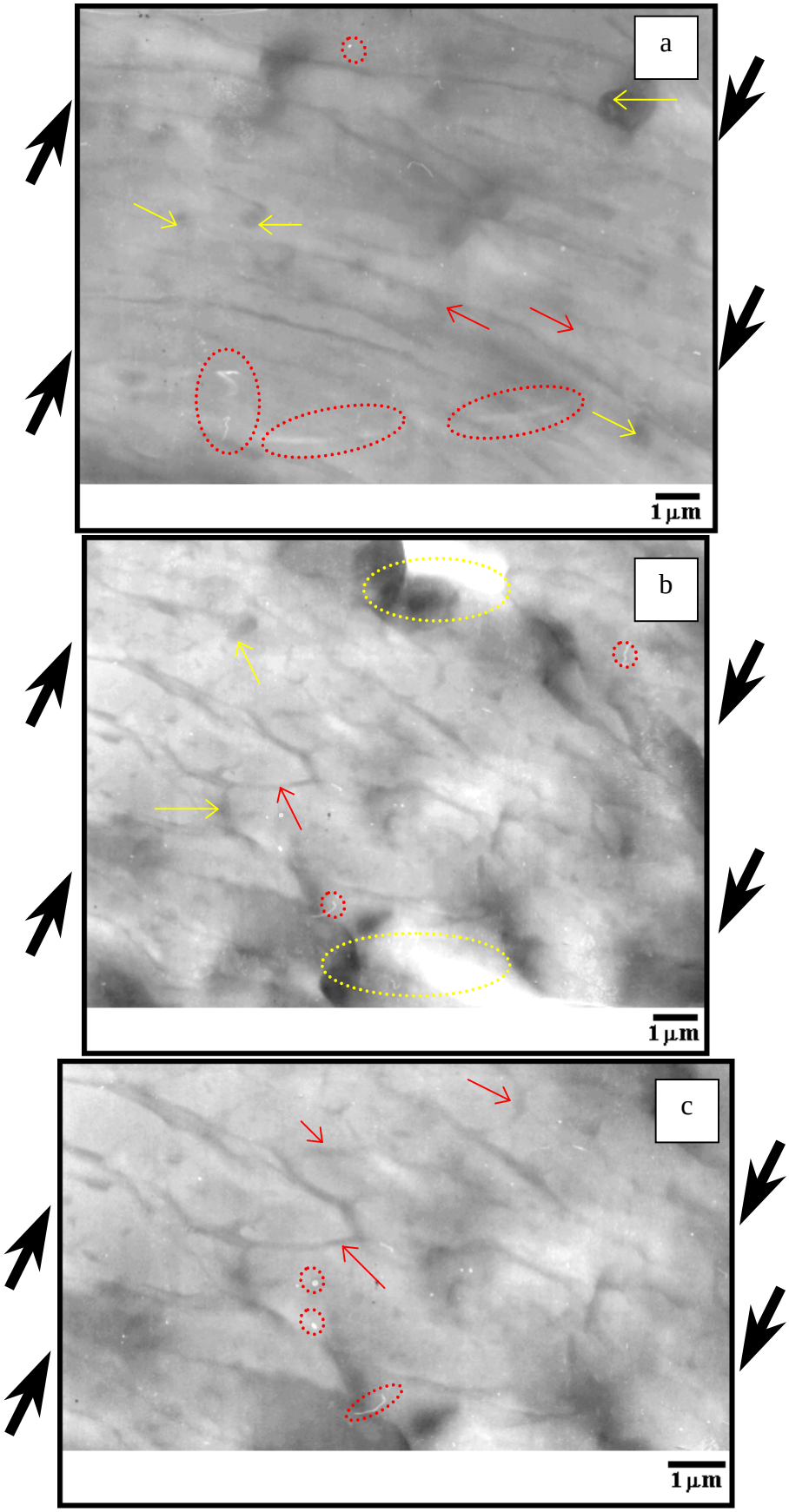

Fig. 6.19. As fig. 6.18,but different areas and magnifications.

As has been seen, the morphology observed in the specimen of blend 50PANIPOL/SBS is consistent with that observed in the cryogenically fractured and etched specimens, respectively. Moreover, the morphologies observed in these TEM micrographs compare well with those observed by Zilberman et al. [23] in other compression moulded PANI-based systems. More generally, the morphologies presented in this section are consistent with those presented in sections 6.4.1 and 6.4.2, thus confirming the hypothesis initially proposed about the formation of layered structures of polyaniline during the compression moulding process.

In summary, the TEM micrographs presented in this section suggest that the morphology responsible for the conduction of electricity through the compression moulded blends consists of a continuous network of polyaniline within the SBS matrix. As suggested by the micrographs, this network should be composed of different morphological arrangements of polyaniline, the main ones including:

- Layered structures. Their continuity degree and content were a function of the content of conductive complex in the blends. Not surprisingly, the higher the content of conductive complex, the larger the number of layered structures and the higher their continuity degree. The maximum thickness estimated for these structures was around 125 nm. However, the occurrence of thicker layers is possible, although to a lesser extent.
- Interconnecting paths. These, interconnecting the polyaniline layers, appeared to be most evident in the specimen of the blend with the highest content of PANIPOL^{TM}. However, although not visible in the micrographs corresponding to the other specimens studied here, it is possible that interconnecting paths of PANI also occur in compression moulded blends with lower contents of conductive complex. This should occur however to a lesser extent.
- Discrete aggregates. These, considerably smaller than the layered structures, appeared to occur in all the specimens studied regardless of the content of conductive complex. Moreover, they seemed to be interconnected by polyaniline paths, especially in the specimen with the highest content of conductive complex. This is expected, since the higher the content of PANIPOL^{TM} in the blends, the higher the probability of the formation of polyaniline paths.

A model describing one of the specimens studied in this work (the one with the highest content of PANIPOL™) is shown in fig. 6.20.

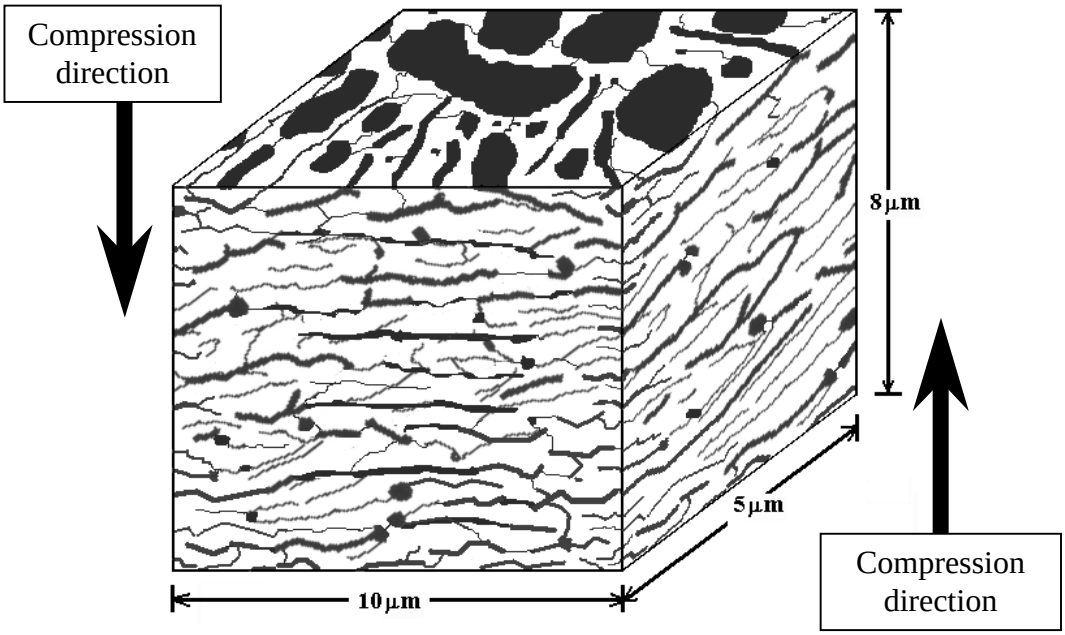

Figure 6.20. Schematic representation of the compression moulded specimen of blend 50PANIPOL/SBS. The black regions represent the polyaniline phase.

Finally, the morphological evidence obtained in this section enables us to establish a corollary: The connectivity degree among the aforementioned morphologies of polyaniline, and hence, the level of conductivity in the blends, are a function of the content of conductive complex. This explains the increase of the conductivity level in the blends with the increase of the PANIPOL™ content.

6.5 CONCLUSIONS.

It was found that compounding in the BRABENDER® batch mixer at 130°C and 15 rpm for 5 min, considerably improved the dispersion of PANIPOL™ in the blends due to the increase of the shear stresses occurring in the melt, which resulted from the increase of the rotors' speed. Additionally, the conductive complex was given more time to mix properly with the polymer matrix.

The relationship between the volume conductivity and content of conductive complex in the blends was found to be characteristic of a percolating system. The percolation threshold seems to occur at a PANIPOL^{TM} content of about 5 wt.%. The results from the conductivity measurements suggested that blending SBS with no more than 20 wt.% of conductive complex could produce an electrically conductive composite with a reasonably good level of conductivity.

The results from the morphological analysis suggest that the morphology responsible for the conductivity in the compression moulded blends consists of a continuous network of polyaniline within the SBS matrix. This network should be composed of different morphological arrangements of polyaniline including, layered structures, interconnecting paths and discrete aggregates. The analysis also proved that the connectivity degree among the aforementioned morphologies is a function of the content of conductive complex, which explains the increase of the level of conductivity in the blends with the increase of the PANIPOL^{TM} content.